Chapter 5. Advanced EXPERIMENTAL TECHNIQUES in Geochemistry

Contributor: Vyacheslav Romanov

"Gentlemen, now you will see that now you see nothing. And why you see nothing you will see presently."
– Quotations by Sir Ernest Rutherford

"Do we see reality as it is? A third of the brain's cortex is engaged in vision. The eye has a retina with 130 million photo-receptors but there are even more neuro-receptors."
– "Decoding Bursts of Light" by Moona Perrotin, Science Rhymes, Australia, 2015.

****

5.1 Heterogeneity challenge

Has anyone wondered why clay is the most ubiquitous weathered geomaterial in earth's crust but we still are in need of developing more and more sophisticated methods and techniques to properly characterize it? The main reason is: it is not well defined; in fact, the variations in local clay structure and composition are virtually infinite. This is caused not only by differences in primary inorganic components of soil but also by historical changes in the local environments. When magma (which is a high-temperature, high-pressure reactive multicomponent system, involving multi-phase eutectics, solid solutions, and dissolved water) incongruently crystallizes upon cooling, it forms igneous rock, the principal constitutive material of the planet's crust. Depending upon the surroundings and the rate of cooling, a great variety of textures and compositions of igneous rock can be formed. When crystallization is complete, the result is a solid mass of interlocking crystals of different sizes. The major structural elements of this rock are silicate groups, SiO_4^{4-} tetrahedra interspersed with mutually soluble metal (commonly, Al, Fe or Mg) cation substitutions, which tend to polymerize by sharing one or more oxygen atoms at the adjacent tetrahedral vertices. Higher degrees of polymerization are associated with higher Si:O ratios and smaller fractions of the foreign metal inclusions. Positive ions that are too large, too small, or too highly charged to be accommodated in silicate structures remain in magma as it solidifies, and form solid minerals during the later stages of cooling. All the silicates are molten at about 1200°C and all are solid when cooled to about 600°C. Consolidation of the solidified geological materials caused by weathering, chemical and biological processes in the pedosphere produces sedimentary rocks (shale, sandstone and limestone).

The primary inorganic components of soil are sand and silt particles that come directly from the parent rocks. This fraction is dominated by quartz and feldspars (aluminosilicates). However, under the influence of heat and pressure, particularly at tectonic plate boundaries, solid crustal material may

undergo partial or complete re-melting, followed by cooling and transformation into metamorphic rocks such as quartzite and mica. The secondary soil components such as clays are formed by chemical changes within the soil itself or in the sediments from which the soil is derived (Chapter 4). Clay is a sedimentary rock made of tiny particles which come from the weathering of other rocks and minerals. The particles can be transported by rivers or ice and then deposited. Soil is a product of the interaction of water, air, and living organisms with exposed rocks or sediments at the earth's surface. A typical soil contains about 45% inorganic solids and 5% organic solids by volume. Water and air each make up about 20-30%. A simple way of classifying soils is based on the relative quantities of clay, silt and sand in the solid component (Figure 5-1) separated by the grain size (as specified by the U.S. Department of Agriculture). Several grain-size scales are in use, but the Udden-Wentworth scale (commonly called the Wentworth scale) is the one that is most frequently used in geology.

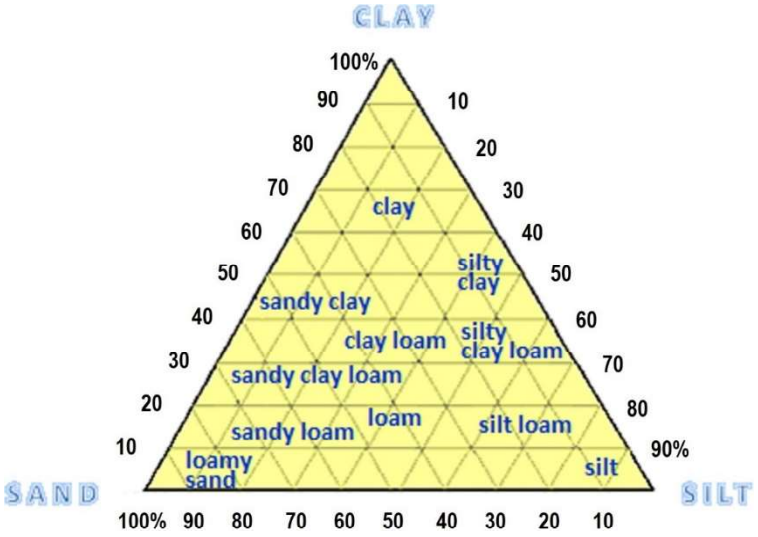

Figure 5-1. Soil classification diagram (Udvardi, et al., 2014)

The ion-exchange properties of clays help to maintain the pH balance of soils, through the exchange of H^+ and cations such as Ca^{2+}. The soil pH, in turn, strongly affects the solubility of cations. Organic matter of soil consists of living organisms such as bacteria and fungi as well as of fulvic and humic acids in association with a variety of smaller organic molecules. Both acids are polyelectrolytes strongly interacting with inorganic ions. Once organic carbon gets incorporated into humic substances, it is locked into a slow (hundreds of years) recycling process. Organic matter binds to the cation components of clay colloids thus acting as cementing agents of soil. The organisms' activity significantly affects the gas-phase composition of soil, thus resulting in oxygen depletion, generation of CO_2 concentration within soil pores at the levels of 5 to 50 times greater than in the atmosphere, and under conditions of poor aeration (controlled by water) substantially increased concentrations of the secondary gaseous components such as N_2O, NO, H_2, CH_4, C_2H_6, and H_2S. Soil water is held by capillary action and adsorption. The water binding strength is traditionally expressed in terms of pressure or "tension" that would be required to force the water out of soil. The capillary pressure in soil varies over a range of

0.01-3.2 MPa (plants can produce osmotic pressure of about 1.5 MPa). Water in excess of the capillary capacity ("gravitational" water) fills larger voids and reduces soil aeration.

Weathering of rocks at the earth's surface is a complex process involving both physical and chemical changes: dissolution, hydration, hydrolysis, reaction with carbonic acid, and oxidation. Among the main causes of physical weathering are the abrasive action of windborne material and glacier movements, rapid temperature changes promoting fracturing by differential expansion, and penetration of water into the voids, with its subsequent freezing. Expansion of water upon freezing can exert pressure of up to 15 MPa, more than the tensile strength of a typical rock. In chemical weathering, the reaction products are not well characterized, thermodynamic data is lacking and the reactions are not entirely understood. The problem with quantifying it in the laboratory is that such reactions occur very slowly and may never reach equilibrium. The rocks that crystallized from magma at higher temperatures (Ca-feldspar and olivine) tend to weather more rapidly than the rocks with lower melting temperature (Figure 5-2). In general, sodium, calcium and magnesium seem to leach before potassium and silicon, while iron and aluminum can only be released very slowly. Individual rates depend on the structural units containing the element and vary with grain size and conditions of the ambient environment. Chemical weathering of rock minerals generally occurs more rapidly in hot, humid climatic regions.

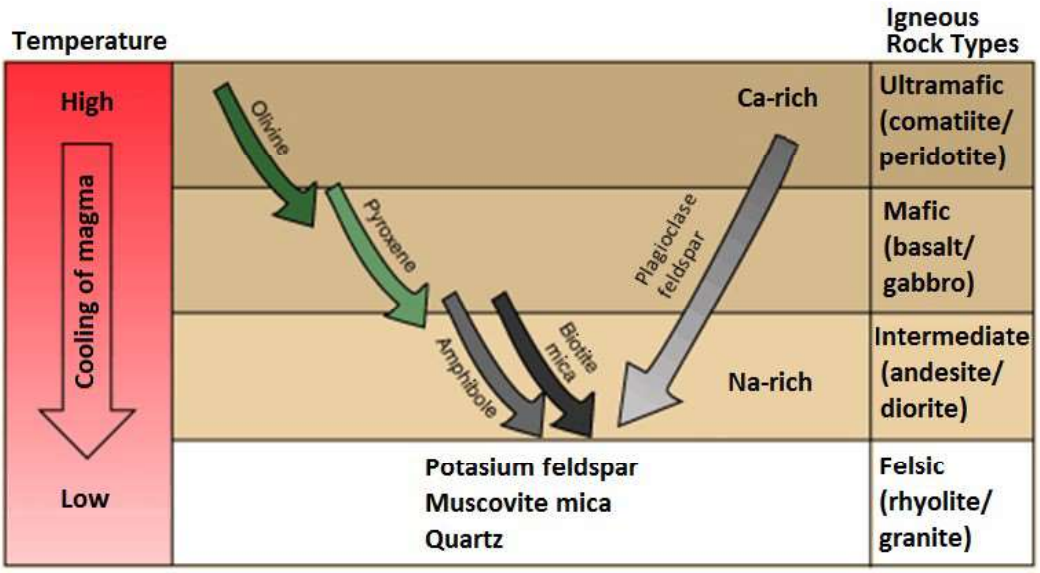

Figure 5-2. Lutgens and Tarbuck's (2014) perspective of the N.L. Bowen's reaction series (originally patterned by Carl R. Nave)

Mineral dissolution usually results in ionic species, some of which may react with water to yield acidic or alkaline solutions. Dissolution of silica, however, results in the neutral species of H_4SiO_4. Reactions involving hydration and dehydration are associated with minor free-energy changes and hence reversible under slightly different conditions. Solid carbonates tend to dissolve in acidic solutions, including those produced when atmospheric carbon dioxide dissolves in water. Thermodynamics can predict the most stable oxidation state of metal ion under given conditions of pH and oxidant

concentration. However, the reaction mechanisms tend to be uncertain for a variety of reasons: the reactant and product can exist in various states of hydration and the dissolved species are a mix of poly-cations and complexed species undergoing oxidation.

The chemical composition of rocks tends to be complex and variable as well; often it can only be defined in a more precise manner at the structural level—traditionally, in terms of the mass percent of oxides of the elements present in the rock, even though the oxides may not be present as structural units. In the chemical analysis of rocks, oxygen is generally not determined separately, though neutron activation analysis may be utilized to determine its content quite accurately; it is expected to combine stoichiometrically with the other elements, including hydration and structural 'water' (H_2O^- that evolves below 105 °C and H_2O^+ that evolves between 105–1000 °C). In clay studies, even the same locality may contain a multitude of subtly different minerals, with substantial variations in mineral assemblage and the composition of individual clay minerals. As a result, the data from different laboratories on ostensibly the same clay may not be comparable. Several coherent attempts have been made, however, to collect samples of representative clays, homogenize and analyze them, and publish the baseline study results. As any processing may affect the material properties, it is necessary to carefully take into consideration its implications as well as the primary objectives of a given research, to properly assess the tradeoffs and choose the most appropriate options. For example, even partial homogenization (sample scale uniformity) alters clay fabric and cation exchange; and drying may result in irreversible changes in lamellar or globular microcrystalline aggregation.

5.2 Preliminary sample characterization

The basic clay properties that are conventionally characterized are its geological origin, chemical composition, structural patterns, layer charges, cation-exchange capacity, thermal behavior, and colloid and surface properties. Although geological origin descriptions may seem somewhat speculative, they provide an important foundation for developing clay models (a combination of fundamental theory and statistics) that are inevitably called upon for interpretation of the experimental data collected on heterogeneous samples. Chemical analysis is the most essential step in mineral analysis; however, it usually follows the structural analysis, in order to identify the major crystalline phases and impurities which can also be removed by selective dissolution—without removing the impurities (such as crystalline silica) it is not possible to accurately derive the formation-specific structural composition (e.g., of the Gonzales County, TX smectite-rich bentonite STx-1). If purification is required, it must be done in a manner that does not significantly alter the physical or chemical properties of the sample. As mentioned in Chapter 4, clay minerals are usually fine-grained (<2 μm); this physical property can be utilized to separate them from coarse-grained minerals (such as quartz, feldspar, or calcite). The textures of smectite, illite, and mixed layer I/S, which are important mineral components in sediments and soil, are very different in sandstones, bentonites and other rock type. However, some characteristics of the clay particles and their interfaces could be altered during the separation and subsequent evaporation due to proton exchange and surface charge alteration.

An important problem in clay mineralogy has been the understanding of the structure of clay particles and how that structure is perceived by XRD of sedimented (onto glass slides) aggregates. The

sedimented aggregates consisting of clay suspensions dried onto a flat surface (see section 5.3) are useful because the preferred orientation of the sheet-like clay particles enhances the $d_{00\ell}$ diffraction maxima, thus resolving the diagnostic (c*-axis) dimension of various clay minerals. It is generally accepted that clay particles are of the order of 0.1 μm in length and width (i.e., in a and b dimensions) but the number of associated unit-cells (*N*) along the c direction can be debatable. This is particularly true for smectite, illite, and interstratified clays (e.g., I/S – see Chapter 4). The controversy arises from the relationship between the shape and intensity of the XRD maxima and *N* as defined by the interference function (Guthrie & Reynolds, 1998). For the Debye-Scherrer geometry:

$$B = K\lambda / N\, d \cos\theta \tag{5.1}$$

where *K* is a dimensionless particle's shape-factor with a value close to unity (e.g., 0.89 for a sphere), *d* – the layer spacing, λ – the wavelength of radiation, θ – the Bragg angle, and *B* – the diffraction peak breadth measured in radians 2θ (at half-height). The maxima broaden and their intensity decreases as *N* decreases.

The fp concept (as defined in Chapter 4) assumes that particles separated for XRD analysis were either separate units (stacks) in original rocks, or thin sub-units of MacEwan crystallites (thick stacks) with incoherent and coherent / semi-coherent (e.g., turbostratically stacked owing to rotational disorder) interfaces (Peacor, 1998; Guthrie & Reynolds, 1998). Cleavage is assumed to occur on the incoherent interfaces—e.g., polar, smectite-like terminations (acting as smectite interlayers) in I/S systems—thus separating the stack into fp's within each of which the interfaces are coherent (illite-like). Although the term "coherent" was not used in the original definition, the crystallographic implication of experimentally observed single-crystal hk0 patterns is that the layers be related by three-dimensional (3D) periodicity (rotations of multiples of 60° around the c* axis, which occur periodically) or by stacking faults that are random variations in the sequence of 60° rotations (Peacor, 1998).

> *One of the touchstones of crystallography, Nicolaus Steno's (born Niels Stensen) Law of Interfacial Angles (1669) concerning the appearance of crystals, reflects a regular arrangement of atoms from which a notion of 3D periodicity is derived.*

This paradigm may cause confusion (regarding the usage of the terms crystal, crystallite, coherent domain, particle, and layer) because a coherent 1D arrangement of layers is no longer a mixed-layered crystal. The concept's evolution to account for experimental (TEM) evidence of lattice-fringe images—the spacing of such set of fringes is proportional to the mineral's lattice spacing when the corresponding lattice planes meet the Bragg condition, viewed in direct space—and the polar character of I/S (Nieto & Cuadros, 1998) has brought it closer to the traditional mixed-layer view in MacEwan or Markovian interpretive models (Reynolds, 1980) which consider the I/S crystallites as composed of smectite and illite layers (also with polar character)—the remaining difference lying only in the crystallographic (3D) coherence across fundamental particles (particularly, across smectite interlayer).

To resolve the fp – MacEwan crystallites controversy, it was necessary to observe the above coherence while using samples of sedimentary origin that are indeed representative of sedimentary sequences, and to take into account clay heterogeneity, which is implicit in the Markovian statistics used to model

I/S (Drits, 1987) and was described in the mathematical decomposition of diffraction patterns (Lanson & Champion, 1991). The consensus is that I/S mixed-layer (ML) stacking is generally different from complete disorder ($1M_d$) polytypism (Ahn & Buseck, 1990).

The earlier (prior to 1990) TEM investigations of ion-milled specimens showed large regions containing clay mineral lattice fringes with periodicities that were suggested as representing mixed layering of illite and smectite. However, the lattice-fringe images do not contain information regarding structural coherency between stacked 2:1 layers. To address this problem, there are several methods available, in addition to the determination of coherent scattering domain size (*N*) from XRD patterns (Eq. 5.1): Bertaut-Warren-Averbach (BWA) analysis of XRD patterns collected on I/S intercalated with high molecular weight polyvinylpyrrolidone; counting layers on high-resolution TEM (HRTEM) lattice-fringe images; Pt-shadowing; and calculation of the average number of fundamental particles per MacEwan crystallite by using the fixed cation content (Mieunier, et al., 2000).

Electron diffraction patterns and lattice images (interference patterns between the direct and diffracted beams, viewed in direct space) are two forms of data which allow crystallographic analysis in TEM. Two types of electron diffraction patterns in TEM are referred to as selected area electron diffraction (SAED) and convergent beam electron diffraction (CBED). Nano-diffraction using CBED is useful in studies of very small crystallites. Kikuchi diffraction (Nishikawa & Kikuchi, 1928) and the crystal orientation-dependent fringe-visibility maps (Fraundorf, et al., 2005) can be realized via both SAED and CBED. Proof of coherency between two or more contiguous interlayers occurs where the corresponding 001 lattice fringes are cross-cut by non-001 (e.g., 020) fringes included in the objective lens aperture; then those 001 layers must have the non-001 plane in common and be related by multiples of 60° rotation around c* (i.e., they must be coherent interfaces). As the focal conditions are different for imaging the 001 fringes and cross fringes, through-focus series of images are obtained, normally from 100 nm under-focus to 100 nm over-focus. Coherency across even smectite interlayers is commonly demonstrated in original rocks by: TEM lattice-fringe images with “cross-fringes”; euhedral crystals of I/S, smectite, and illite; and SAED patterns with discrete, but non-periodic hkl reflections—In the latter case, cross fringes are the Fourier transform of ill-defined, non-00ℓ reflections in SAED patterns (Peacor, 1998).

SAED pattern must include **c*** (in reciprocal space), an orientation promoted by preparation of TEM samples as thin sections normal to bedding, that is, with (001) planes parallel to the electron beam (Dong & Peacor, 1996). The second vector must then lie in the **a***–**b*** plane and the rotation around **c*** may become either **a*** or **b*** or one of their pseudo-symmetrically-related, 60° rotation-equivalents. Although **a***(**b***) and its rotation-equivalents have nearly equal d-values, the angle between **c*** and the equivalents is different from the one between **c*** and **a***(**b***). TEM images show that montmorillonite particles exhibit thin-plate and curly-flake morphologies (Roberson, et al., 1968; Nadeau, et al., 1984), with long, parallel but undulated layers, which complicates the 3D image reconstruction (Malla, et al., 1993).

Caution must be exercised when interpreting the XRD and TEM results. The dispersion processes for XRD and TEM analyses would easily disarticulate originally-undisturbed crystallites into “fundamental particles” with no geological meaning with respect to the original sample (Nieto & Cuadros, 1998). While

fp observed in particles separated for XRD are assumed to be related by incoherent interfaces in original rocks, implying that the sites of coherent and incoherent interfaces in separates are identical to those in original rocks; that must depend critically on the severity of sample treatment (Peacor, 1998). It has been shown that 3D periodicity of I/S can be induced through smectite interlayer-ion saturation and thermal effects. HRTEM methods of sample preparation require that the bulk-rock specimen be sectioned, polished, and subjected to ion-milling (a beam of high-energy ions). In the high-vacuum environment during the latter procedure, effects of ion-milling illitic or micaceous specimens could result in potassium fixation in nearby ion-exchange sites, and increases susceptibility to alteration of three-dimensional periodicity (Nadeau, 1998).

As the abundance of any mineral is determined by the availability of its constituent elements in the Earth's crust, its chemical composition combined with the mineralogical information is important in shedding the light on the mineral's origin and transformation history. The clay elemental composition analysis by a combination of atomic absorption (AA) and atomic emission (ICP/ICP-MS or flame emission, particularly for alkali metals) spectroscopy methods is routinely performed following the microwave-assisted acid digestion, and sometimes after the subsequent neutralization. ICP-MS (i.e., inductively-coupled-plasma mass-spectrometry) is ideally suitable for rapid qualitative elemental analysis of clays and other geomaterials; however, the quantitative analysis requires the use of external calibration standards and corrections applied for mass-dependent matrix effects, mass spectral interferences, and drift. The quantities of multivalent element fractions (such as Fe^{3+} vs Fe^{2+}) are determined separately. The main principle of atomic emission spectroscopy—a unique emission spectrum corresponding to a unique atomic structure—is utilized in a variety of spectroscopic techniques with different excitation sources (electron beam excitation in electron microscopes; X-ray beam excitation in X-ray fluorescence spectrometers) and emission spectra (e.g., Auger electron spectroscopy). Accurate estimation of the elemental composition from the measured X-ray emission spectrum also requires the application of quantitative correction procedures (matrix corrections for the emitted X-rays' re-absorption by the sample). Laser-induced breakdown spectroscopy (LIBS) is another type of atomic emission spectroscopy which uses a highly energetic laser pulse as the excitation source; it was employed to identify various phyllosilicates such as Martian clay analogs (Humphries, et al., 2011).

Thermal analysis involving a dynamic phenomenological approach can also be used to study solid state reactions (chemisorption, reduction/oxidation, desolvation/dehydration, and decomposition) and phase transitions (crystallization, glass transition, melting and sublimation, vaporization, absorption, adsorption, and desorption) by monitoring a variety of physical properties: mass in thermo-gravimetric analysis (TGA), mass changes as function of pressure in pressurized TGA (PTGA), temperature difference in differential thermal analysis (DTA), heat difference in differential scanning calorimetry (DSC), gaseous decomposition products in evolved gas analysis (EGA/TGA-MS), deformations and dimension in thermo-mechanical analysis, and volume in dilatometry. Often different properties can be measured simultaneously. For example, TGA-MS can be used to characterize desorption of various species (water and adsorbed gases) from geomaterials; alternatively, CO_2 coulometer can be used for total carbon determination by measuring the amount of CO_2 evolved, when coupled with thermal decomposition of the sample (by heating up to 1000 °C) or for carbonate carbon determination by using complementary

acid digestion technique. For gas or supercritical fluid sorption studies, specialized sorption isotherm techniques of quantitative manometric or gravimetric measurements (convoluted by sample swelling) can be combined with semi-quantitative Raman and infrared (IR) spectrometry studies.

IR spectroscopy is a powerful tool for mineralogical, composition, and structural analysis of clay (Madejová, 2003). In combination with a polarizer placed between interferometer and the IR reflectance cell, it provides enhanced capabilities to study preferred orientation of clay layers and even specific chemical bonds; which is particularly useful for monitoring and analyzing clay–fluid interactions (Amarasinghe, et al., 2008; Ras, et al., 2003; Johnston, et al., 1992). Optical microscopy, on the other hand, can be used for preliminary characterization of the lateral swelling of clay aggregates to complement the X-ray diffraction (XRD) studies. Laser scanning microscopy was used to investigate bentonite swelling in NaCl solution (Suzuki, et al., 2005).

5.3 Analysis of crystalline phases

Qualitative identification of the crystalline phases in multicomponent clay samples can be performed using conventional laboratory XRD methods and equipment (Chapter 4). The amount of sample available and what a researcher hopes to reveal about the sample will determine how the sample is prepared and/or mounted; for example, small specimens of oriented clay particles can be mounted on the zero background (off-axis-cut) quartz plates to improve signal-to-noise ratio. Semi-quantitative evaluation of the mineral abundances (amorphous components are not quantified, though the recent development of techniques that interpret both Bragg and diffuse elastic scattering has extended the use of XRD to amorphous materials) requires the use of external standards, accounting for variations in degree of preferred orientation of the crystallites (for the random mount) or the finite sample thickness (for the oriented samples), Lorentz-polarization effects, and relative humidity during the analysis. The latter is particularly important for smectite samples whose basal 00ℓ-diffraction pattern varies as a function of numerous factors, which prompts some researchers to explore the environmental cell options. High-pressure rated cells are particularly useful for studies on clay interaction with greenhouse gases for as long as the cell's window is sufficiently transparent and does not convolute the observed diffraction patterns. Hence, they may not be suitable for all laboratory X-ray machines and may even require the use of synchrotron (Kulipanov, 2007) light-source beamlines.

Synchrotron radiation can be advantageous to laboratory sources for several reasons: orders of magnitude higher brightness and intensity (for 3rd generation sources, brilliance larger than 10^{18} photons/s/mm^2/mrad^2/0.1%BW, where 0.1%BW is a bandwidth of fx10^{-3} centered around frequency f; and for 4th generation, X-ray free electron lasers, brilliance larger than 10^{24} photons/s/mm^2/mrad^2/ 0.1%BW); higher collimation; higher degree of polarization; lower emittance (product of source cross-section and solid angle of emission); larger wavelength tunability (use of monochromators); pulsed light emission (pulse durations may be below one nanosecond in 3rd generation sources and close to picoseconds in 4th generation sources) allows ultra-fast time-resolved studies.

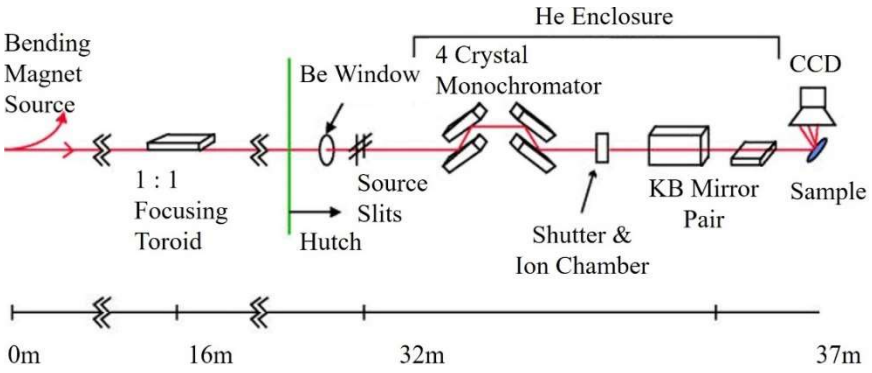

Figure 5-3. Schematic layout of a Beamline at the Advanced Light Source, Berkeley Lab (http://www-esg2.lbl.gov/microdif/beamline733.htm accessed May 19, 2017)

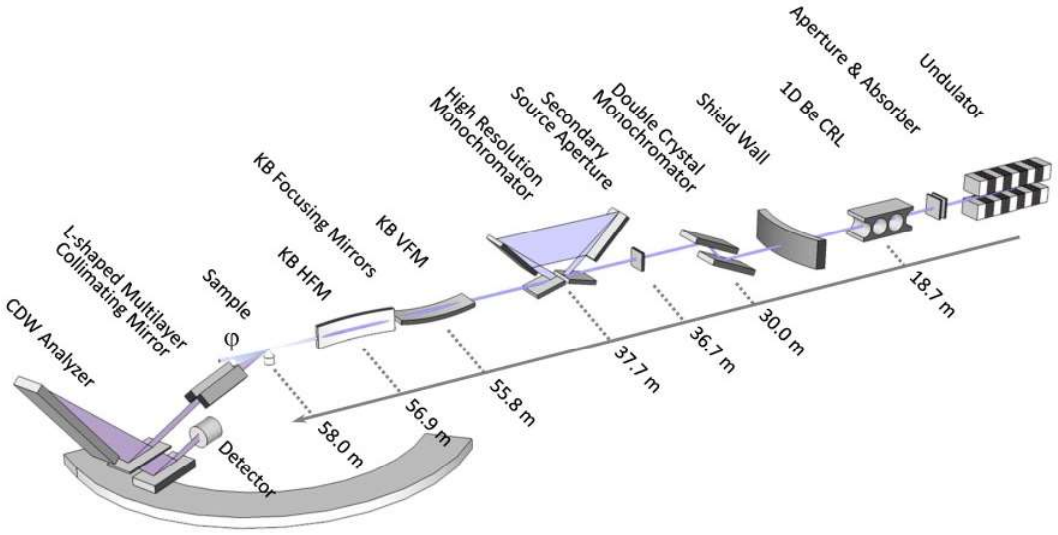

Figure 5-4. Inelastic X-ray Scattering Beamline at Brookhaven National Laboratory world-brightest light source, NSLS II (Suvorov, et al., 2014); CRL = compound refractive lenses, KB = Kirkpatrick-Baez focusing with independent vertically & horizontally focusing mirrors (VFM & HFM), CDW = charge-density-wave phase deformation

The advanced light-source (beamline) facilities (see examples in Figure 5-3 and Figure 5-4) are naturally equipped with a variety of probes that fall into three broad categories: diffraction and scattering (like X-ray reflectivity, including resonant anomalous and standing wave) techniques, spectroscopy (X-ray and low-energy) and imaging (X-ray and IR). Simultaneous recording of both small and wide angle X-ray scattering (SAXS and WAXS) in combination allows users to probe length scales ranging from a few Angstroms to several micrometers, with high resolution. HRTEM in conjunction with SAXS can be used to study the effect of interlayer cations, hydration state, and applied pressure on organization of clay layers including the size of crystallites. The unique properties of synchrotron radiation are its high collimation and coherence, high flux and brightness (brilliance) essential for SAXS studies of oriented samples, continuous (high resolution, tunable) spectrum that enables studies of anomalous SAXS close to the

absorption edges of the element. Synchrotrons' major advantages over laboratory XRD is high-volume event counting statistics (millions of counts in just a few seconds)—in reflection (Bragg-Brentano) and transmission (Debye-Scherrer) modes; transmission geometry, fast data acquisition and high-frequency sample spinning contribute to reduced preferential orientation effects; polarization and the pulsed nature of these sources can also be harnessed in special experiments.

Advances in developing environmental pressure cells with X-ray transparent windows (Giesting, et al., 2012; Loring, et al., 2012) produced a number of high-pressure X-ray diffraction reactors which allow conducting in situ observation of swelling clay as it interacts with active gases/fluids like CO_2. Such reactors can be used to precisely control humidity as well as simultaneously observe infrared spectra of the gas and solid phases, along with XRD patterns. Controlled humidity experiments are particularly important for highly hygroscopic samples like clays.

5.4 Element-specific advanced analytic techniques

Molecular structure in the clay interlayer has been studied experimentally using a variety of techniques: IR spectroscopy, incoherent neutron scattering, nuclear magnetic resonance (NMR) spectroscopy, dielectric relaxation, neutron and X-ray diffraction, and others (Sposito & Prost, 1982). Among the chemical element-specific, soft X-ray/vacuum-ultraviolet spectroscopy techniques based on the measurement of absorption, transmission, or reflectivity of a sample as a function of the incident photon's energy, electron photoemission (XPS/UPS), fluorescence and inelastic photon scattering (viable only at brilliant synchrotron sources) are most common. XPS (Figure 5-5) was reported to detect carbonate formation near clay surfaces, though it is difficult to resolve the broadened (due to differential surface charging) chemical shift distributions and identify specific kind of carbonate species among others or to detect whether they are in the interlayer or at the external surfaces. There are several semi-quantitative XPS depth-profiling methods, including ion etching, surface charging, angle-resolved (for oriented samples) and QUASES (developed by Sven Tougaard) methods, but all suffer from various limitations. The ion beam etching (for depth profiling) leads to destructive chemical and topographical modifications; hence difficulties with data interpretation. 3D atom probe tomography (APT) is an alternative technique for imaging and chemical composition analysis at atomic scale, based on progressive electrostatic-field evaporation of atoms from a sample prepared in the form of a very sharp tip, time-of-flight detection and 3D reconstruction.

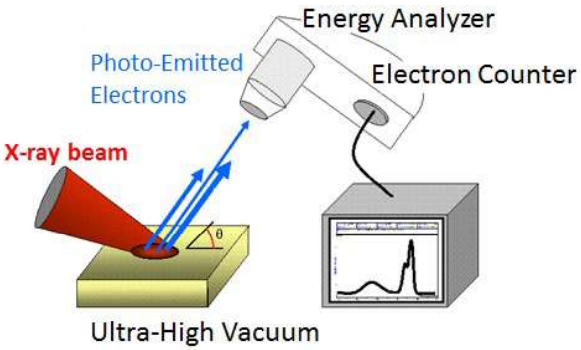

Figure 5-5. X-ray Photoelectron Spectroscopy (wikimedia)

Non-destructive techniques that are complementary to crystallography are electron microscopy (EM) and NMR spectroscopy for structure determination and the study of dynamics. Advanced methods of non-destructive imaging include soft X-ray imaging (with the use of photon or electron optics to achieve high spatial resolution) and hard X-ray tomography (with raster scanning of the sample through the illuminated spot). X-ray tomography can be performed in situ (with the sample placed in controlled gas and temperature environment). Hard X-ray imaging nondestructively visualizes samples, frequently the internal or hidden components of the samples. The contrast can be due to changes in absorption, elemental composition, or refractive index of the sample.

The X-ray standing wave (XSW) technique, briefly mentioned in section 5.3, provides another non-destructive element-specific structural probe by using X-ray reflectivity (XR) setup to generate a "two-beam" interference field that in turn induces a spatial dependence to spectroscopic (fluorescence or photoelectron) yields from atoms within the field. XR is extremely powerful for obtaining in-situ information about structural properties of surfaces and interfaces on the atomic scale, with high spatial resolution and chemical selectivity (Fenter & Lee, 2014). Despite insensitivity toward hydrogen atoms, the X-ray techniques have proven their efficiency in assessing the clay interlayer electron density profiles and in determining the conditions with minimum hydration heterogeneity required for neutron diffraction (ND) experiments.

Advancements in small-angle scattering of neutrons—interacting with atom cores—provide more reliable data for indirect determination of the physical dimensions of clay particles, compared to more traditional techniques like electron-optical birefringence, ultra-centrifugation, viscosity, and UV-Vis (ultraviolet-visible) light scattering (Nadeau, 1985). ND also represents a step forward in the validation of clay and H_2O models, because contribution to the diffracted intensities of interlayer species increases from ~25% for X-ray to ~40% (using H_2O) and ~47% (using D_2O) for neutron diffraction (Ferrage, et al., 2011). However, strong divergence of neutron beams broadens 00ℓ reflections and leading to an apparent decrease of the coherent scattering length (from about 12-16 layers for XRD to 5-7 for ND). This, in combination with short wavelength and large angular steps, makes calibration of experimental data difficult to perform; and modification of ND reflection intensity distribution induced by the presence of minor hydration heterogeneity may lead to erroneous assessment of the interlayer models.

> *A comprehensive dataset provided by a combination of the XRD and ND can be used for advanced model refinement, by utilizing a technique devised by Hugo M. Rietveld (1969) for use in the characterization of crystalline materials, to deal reliably with strongly overlapping reflections. Layer stacking faults in clay minerals may hamper the Rietveld refinement and require specific algorithms* (Brigatti & Mottana, 2011).

UV-Vis spectroscopy is not as widely used in chemical-selectivity research because of molecular absorption band overlap. However, UV-Vis spectroscopic measurements are not detector noise limited as are IR measurements. For this reason, advances in phase-, time-, and space-resolution using step-scan as well as rapid-scan spectroscopy were first made in the UV-Vis region and only later followed by the Fourier-transform IR (FTIR). Time-resolved FTIR is a spectroscopic technique whereby transient processes, including non-cyclic (Rammelsberg, et al., 1999) can be measured; with these advances,

transient (in the range of a couple of seconds to nanosecond range) species can be identified from parent species by a specific change in vibrational properties.

Mid- and far-infrared microprobes using synchrotron radiation are used to address heterogeneity problems such as multiple mineral phases in geological specimens and for chemical identification and molecular conformation studies. Infrared radiation from a synchrotron is more intense than that from a conventional laboratory source, but it is still nondestructive. A variety of high-pressure IR cells (transmission, reflectance, and advanced combinations) are available for in situ studies of the interaction between geomaterials and fluids at relevant temperature and pressure conditions. At high concentrations of the active species in the gas/fluid phase, the attenuated total reflection (ATR) is a natural choice to study surface phenomena; it became a routine, high-throughput laboratory technique in combination with FTIR spectrometry, despite the need to de-convolute the spectra. In advanced applications, it can be paired with the transmission technique used to simultaneously monitor concentration of the gaseous water molecules. Similar to X-ray techniques, it can be used to study orientation-dependent properties. Additionally, micro-ATR (in conjunction with microscope optics) imaging has opened up the areas of study that were previously precluded by inadequate spatial resolution of conventional (macro-) ATR cells. This has applications in analyses of heterogeneous samples with small domain sizes. In practice, micro-spectroscopic mapping is limited to 10–15 μm spatial resolution in traditional laboratory settings.

The effects of the ATR technique on observed spectrum are well characterized. The near-field penetration depth is inversely proportional to the wavelength; therefore, the peak intensity is relatively more attenuated on the higher wavelength side of the spectrum. This may cause a skewed baseline, peak's distortion and changes in its position (shifted toward lower wavenumber side, compared to transmission spectra) and intensity, commonly in spectra of the samples with higher refractive index. The observed change in peak width is attributed to the change in refractive index as a function of wavenumbers, which is more prominent in the case of strong absorption and higher refractive index of the prism. In any case, the prism must have a relatively high (compared to the sample) refractive index for this technique to work properly. When using the ATR technique to measure solid samples, it is necessary to press the sample against the prism. If there is any change in the physical state of the sample due to pressure, these changes will be manifested in obtained spectrum.

IR/Raman spectra can serve as a fingerprint for mineral identification, but they can also provide unique information about the mineral structure, the degree of regularity within the structure, the nature of isomorphic substituents, the distinction of molecular water from structural hydroxyl, and the presence of either crystalline or non-crystalline impurities. Most of the spectroscopic studies on source clays (Clay Minerals Society specimens) have been done in mid-IR (MIR) region but some information about structural OH groups and H_2O was gleaned from overtones in near-IR (NIR) reflectance spectra as well. Diffuse reflectance infrared Fourier-transform (DRIFT, Figure 5-6) spectroscopy is most suitable for studies of hydroxyl vibrations of clays in both MIR and NIR regions. Coal and soil samples may also be analyzed by diffuse reflectance as neat powders. To minimize interference effects created by particle sizes (of some larger aggregates) matching the incident IR radiation wavelength, the analyte is mixed

with KBr to obtain high quality DRIFT spectra toward the low-frequency region (for clay powder: below 1200 cm^{-1}); however, interaction between the clay sample and KBr may even occur at room temperature. Diffuse reflectance can also be used to study the effects of temperature by configuring the accessory with a heating chamber. The sample should be loosely but evenly packed in the cup to maximize IR beam penetration and minimize spectral distortions.

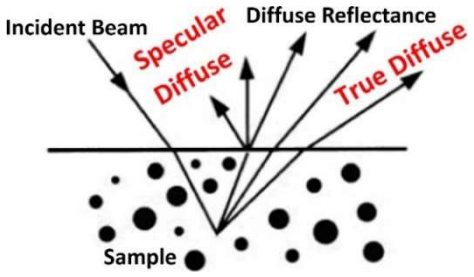

Figure 5-6. DRIFT spectroscopy

An advanced variation of the ATR is nearfield scanning optical (or infrared) microscopy (NSOM) taking advantage of the evanescent waves' perturbation near precision-positioned subwavelength features. For example, in the apertureless (ANSOM) mode of operation (Figure 5-7) such a feature is the atomic force microscope (AFM) cantilever tip. Hence the resolution is limited by the effective radius of curvature and quality of the tip and not by the wavelength of p-polarized illuminating light used in such applications. Lateral resolution of 10–20 nm and vertical resolution of 2–5 nm has been demonstrated for the contrast imaging at a fixed (infrared or visible) excitation wavelength (Romanov & Walker, 2007). As a bonus, AFM is used to measure sub-nano Newton forces (strength of atomic bonding, single-molecule stretching and rupture forces, van der Waals and Casimir-Polder forces, and dissolution forces in liquids)—with demonstrated spatial resolution on the order of fractions of a nanometer.

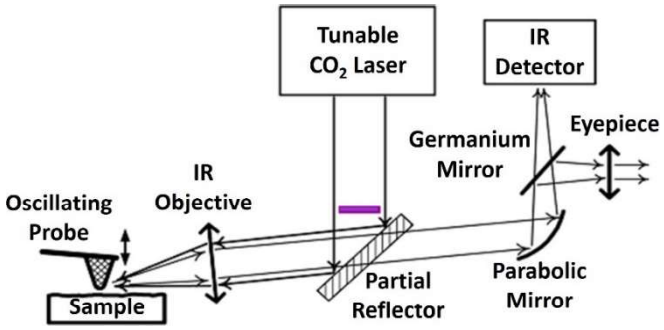

Figure 5-7. Example of ANSOM design (University of Pittsburgh)

Although high-contrast ANSOM images have been observed using infrared (1650-1950 cm^{-1}) laser excitation, the interpretation of the near-field spectral features is not straightforward and generally requires rigorous simulations. Several advancements in experimental techniques and instrumentation (such as second-harmonic detection, homo- and heterodyning, and phase-shifting interferometry)

simplified the methodology and improved the signal-to-noise ratio; but the near-field infrared detection remains in its nascent state and is primarily limited to advanced scientific experimentation.

The above techniques can provide a wealth of information about a variety of the natural materials; and methodology for examination of the structure and composition of minerals keeps advancing rapidly. However, classification of 2:1 phyllosilicates (packets of the discrete layers composed of two tetrahedral sheets coordinated to a central octahedral sheet, with shared oxygens) remains a problem. The scientists still do not fully understand the interactions that occur at the surfaces or interfaces. Clay mineralogists emphasize importance of the layer charge for their characterization—arguably, the most significant characteristic of such minerals. For homoionic clay minerals, the charge distribution between the sheets as well as the total layer charge may be estimated from the occupancy of elements in the tetrahedral and octahedral sheets, based on the structural formula. Determination of the layer charge based on the basal spacing expansion after cation exchange (e.g., with alkylammonium cations of varying chain lengths) proved to be a more practical (albeit time-consuming) approach, as it is not always possible to accurately derive the structural composition due to persistent contaminants. Alternatively, infrared spectroscopy permits semi-quantitative determination of the total layer charge for NH_4^+-exchanged clays via measurement of the NH_4^+ ν_4 deformation band intensity using a calibration curve. However, it is important to remember that any procedure involving cation exchange in solution, with subsequent drying may change the aggregate properties of the specimen.

Differentiation between the octahedral and tetrahedral charges is possible but requires advanced scientific studies tailored to specific mineral structures. For example, saturation of dioctahedral (but not trioctahedral!) smectite with Li^+ and heating at 200–300 °C may lead to migration of the small Li cations towards free octahedral (but not tetrahedral!) vacancies where they neutralize the negative charge imbalance arising from isomorphous ionic substitutions in the structure of octahedral sheet. This experimental evaluation is compromised, to some extent, by the variable (pH-dependent) positive charge of the crystal-edge sites.

When a solid mineral comes into contact with a liquid, its surface acquires an electric charge due to unsatisfied structural charge imbalance, ionization, broken bonds, differential dissolution, and sorption of charged species from the liquid. Generally, behavior of the fine (colloid-sized) solid particles in the solution is controlled by the ζ-potential (the electric potential at the slipping plane that separates mobile fluid from fluid attached to the particle's surface) which indicates the degree of electrostatic repulsion between adjacent, similarly-charged particles in a dispersion.

In practice, researchers tend to modify available experimental techniques to suit particular systems and phenomena under investigation. Frequently, multiple techniques are intertwined in a complex experimental setup to simultaneously collect as much relevant information as possible. Such advances generally go hand-in-hand with advances in conceptual understanding of the experimental observations. In the following chapters, that will be demonstrated on research examples related to interaction of greenhouse gases with clay systems.

Chapter 5 references

Ahn, J. H. & Buseck, P. R., 1990. Layer-stacking sequences and structural disorder in mixed-layer illite/smectite: Image simulations and HRTEM imaging. *American Mineralogist,* 75(3-4), pp. 267-275.

Amarasinghe, P. M., Katti, K. S. & Katti, D. R., 2008. Molecular Hydraulic Properties of Montmorillonite: A Polarized Fourier Transform Infrared Spectroscopic Study. *Applied Spectroscopy,* 62(12), pp. 1303-1313.

Brigatti, M. F. & Mottana, A. eds., 2011. *Notes in Mineralogy, Volume 11, Layered mineral structures and their applications in advanced technologies.* 1st ed. London: European Mineralogical Union and the Mineralogical Society of Great Brittain & Ireland.

Dong, H. & Peacor, D. R., 1996. TEM observations of coherent stacking relations in smectite, I/S and illite of shales; evidence for MacEwan crystallites and dominance of 2M polytypism. *Clays and Clay Minerals,* 44(2), pp. 257-275.

Drits, V. A., 1987. *Mixed-layer minerals: Diffraction methods and structural features.* Bloomington, IN, The Clay Minerals Society, pp. 33-45.

Fenter, P. & Lee, S. S., 2014. Hydration layer structure at solid–water interfaces. *MRS bulletin,* 39(12), pp. 1056-1061.

Ferrage, E. et al., 2011. Hydration properties and interlayer organization of water and ions in synthetic Na-smectite with tetrahedral layer charge. Part 2. Toward a precise coupling between molecular simulations and diffraction data. *Journal of Physical Chemistry C,* 115(5), pp. 1867-1881.

Fraundorf, P., Qin, W., Moeck, P. & Mandell, E., 2005. Making sense of nanocrystal lattice fringes. *Journal of Applied Physics,* 98(114308), pp. 1-10.

Giesting, P., Guggenheim, S., Koster van Groos, A. F. & Busch, A., 2012. X-ray diffraction study of K- and Ca-exchanged montmorillonites in CO2 atmospheres. *Environmental Science and Technology,* 46(10), pp. 5623-5630.

Guthrie, G. D. & Reynolds, R. C., 1998. A coherent TEM- and XRD-description of mixed-layer illite/smectite. *The Canadian Mineralogist,* 36(6), pp. 1421-1434.

Humphries, S. D. et al., 2011. *Investigation of Mars clay analogs by remote laser induced breakdown spectroscopy (LIBS).* The Woodlands, TX, Lunar and Planetary Institute, p. 1851.

Johnston, C. T., Sposito, G. & Erickson, C., 1992. Vibrational Probe Studies of Water Interactions with Montmorillonite. *Clays and Clay Minerals,* 40(6), pp. 722-730.

Kulipanov, G. N., 2007. Ginzburg's invention of undulators and their role in modern synchrotron radiation sources and free electron lasers. *Physics Uspekhi,* 50(4), pp. 368-376.

Lanson, B. & Champion, D., 1991. The I/S-to-illite reaction in the late stage diagenesis. *American Journal of Science,* 291(5), pp. 473-506.

Loring, J. S. et al., 2012. In situ molecular spectroscopic evidence for CO2 intercalation into montmorillonite in supercritical carbon dioxide. *Langmuir,* 28(18), pp. 7125-7128.

Lutgens, F. K. & Tarbuck, E. J., 2014. *Essentials of Geology.* 12th ed. Upper Saddle River, NJ: Pearson Education, Inc.

Madejová, J., 2003. FTIR techniques in clay mineral studies. *Vibrational Spectroscopy,* 31(1), pp. 1-10.

Malla, P. B. et al., 1993. Charge Heterogeneity and Nanostructure of 2:1 Layer Silicates by High-Resolution Transmission Electron Microscopy. *Clays and Clay Minerals,* 41(4), pp. 412-422.

Mieunier, A., Lanson, B. & Beaufort, D., 2000. Vermiculitization of smectite interfaces and illite layer growth as a possible dual model for illite-smectite illitization in diagenetic environments: a synthesis. *Clay Minerals,* 35(3), pp. 573-586.

Nadeau, P. H., 1985. The physical dimensions of fundamental clay particles. *Clay Minerals,* 20(4), pp. 499-514.

Nadeau, P. H., 1998. Fundamental particles and the advancement of geosciences; response to Implications of TEM data for the concept of fundamental particles. *The Canadian Mineralogist,* 36(6), pp. 1409-1414.

Nadeau, P. H., Tait, J. M., McHardy, W. J. & Wilson, M. J., 1984. Interstratified XRD characteristics of physical mixtures of elementary clay particles. *Clay Minerals,* 19(1), pp. 67-76.

Nieto, F. & Cuadros, J., 1998. Evolution, current situation, and geological implications of the "fundamental particle" concept. *The Canadian Mineralogist,* 36(6), pp. 1415-1419.

Nishikawa, S. & Kikuchi, S., 1928. Diffraction of Cathode Rays by Mica. *Nature,* 121(3061), pp. 1019-1020.

Peacor, D. R., 1998. Implication of TEM data for the concept of fundamental particles. *The Canadian Mineralogist,* 36(6), pp. 1397-1408.

Rammelsberg, R., Boulas, S., Chorongiewski, H. & Gerwert, K., 1999. Set-up for time-resolved step-scan FTIR spectroscopy of noncyclic reactions. *Vibrational Spectroscopy,* 19(1), pp. 143-149.

Ras, R. H. A. et al., 2003. Polarized Infrared Study of Hybrid Langmuir−Blodgett Monolayers Containing Clay Mineral Nanoparticles. *Langmuir,* 19(10), pp. 4295-4302.

Reynolds, R. C., 1980. Interstratified Clay Minerals. In: G. Brindley & G. Brown, eds. *Crystal Structures of Clay Minerals and their X-ray Identification.* 3rd ed. London: Mineralogical Society, pp. 249-304.

Rietveld, H. M., 1969. A profile refinement method for nuclear and magnetic structures. *Journal of Applied Crystallography,* 2(2), pp. 65-71.

Roberson, H. E., Weir, A. H. & Woods, R. D., 1968. Morphology of Particles in Size-Fractionated Na-Montmorillonites. *Clays and Clay Minerals,* 16(3), pp. 239-247.

Romanov, V. & Walker, G. C., 2007. Infrared Near-Field Detection of a Narrow Resonance Due to Molecular Vibrations in a Nanoparticle. *Langmuir,* 23(5), pp. 2829-2837.

Sposito, G. & Prost, R., 1982. Structure of water adsorbed on smectites. *Chemical Reviews,* 82(6), p. 553–573.

Suvorov, A., Cai, Y. Q., Sutter, J. P. & Chubar, O., 2014. *Partially coherent wavefront propagation simulations for inelastic x-ray scattering beamline including crystal optics. In Proc. SPIE 9209, Advances in Computational Methods for X-Ray Optics III.* Bellingham, WA, SPIE, p. 92090H.

Suzuki, S., Prayongphan, S., Ichikawa, Y. & Chae, B. G., 2005. In situ observations of the swelling of bentonite aggregates in NaCl solution. *Applied Clay Science,* 29(2), pp. 89-98.

Udvardi, B. et al., 2014. Application of attenuated total reflectance Fourier transform infrared spectroscopy in the mineralogical study of a landslide area, Hungary. *Sedimentary Geology,* Volume 313, pp. 1-14.